PNAS
www.pnas.org

Supplementary Information for:

Development and validation of a potent and specific inhibitor for the CLC-2 chloride channel

Anna K. Koster[a,b], Austin L. Reese[c], Yuri Kuryshev[d], Xianlan Wen[b], Keri A. McKiernan[a], Erin E. Gray[a], Caiyun Wu[d], John R. Huguenard[c]*, Merritt Maduke[b]*, J. Du Bois[a]*

[a]*Department of Chemistry, Stanford University, Stanford, CA 94305, USA*
[b]*Department of Molecular & Cellular Physiology, Stanford University School of Medicine, Stanford, CA 94305, USA*
[c]*Department of Neurology & Neurological Sciences, Stanford University School of Medicine, Stanford, CA, USA*
[d]*Charles River Laboratories, Cleveland, OH 44128, USA*

***Corresponding Authors:** Justin Du Bois, jdubois@stanford.edu**;** Merritt Maduke, maduke@stanford.edu**;** John R. Huguenard john.huguenard@stanford.edu

This PDF file includes:

Figures S1 to S5
Tables S1 to S4

Other supplementary materials for this manuscript include the following:

Dataset 1: Compound library screening results
Dataset 2: PDSP and anion channel screening
Dataset 3: Chemical synthesis and characterization

Supplementary Figures

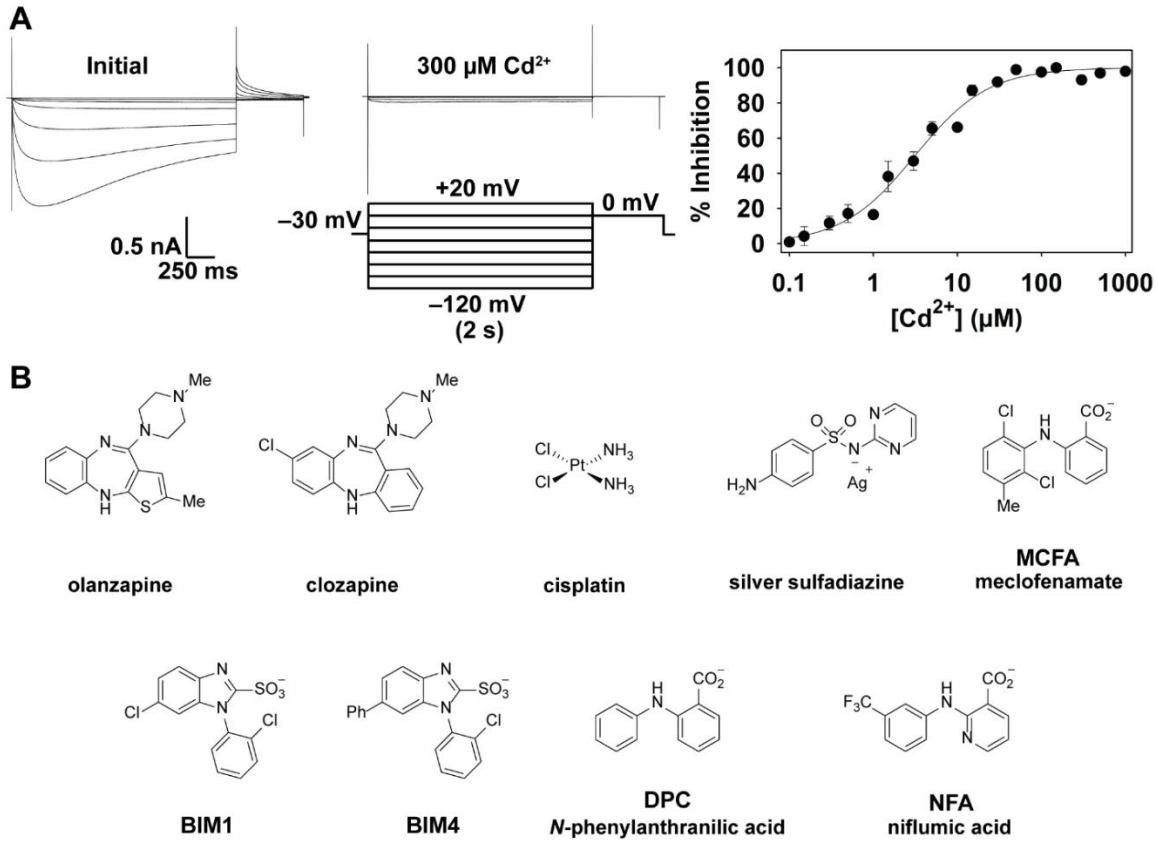

Fig. S1. CLC-2 assay on the IWB and identification of 'hit' compounds. (**A**) Assay development. *Left:* Representative human CLC-2 currents on IWB measured before (left) or after (right) treatment with positive control Cd^{2+} in response to the voltage protocol shown. The current decay at negative voltages, which is not seen in manual patch-clamp recordings (**Figure 4C** and references (1–3)) or in a different automated patch-clamp platform (PatchXpress, unpublished data), is likely due to the differences in the intracellular solution, which in this case includes a mixture of Cl^- and F^-. *Right:* Summary data for inhibition of CLC-2 by Cd^{2+} (± SEM, n = 4–32; IC_{50} = 3.1 ± 0.3 µM). Inhibition was calculated using the maximum current at –120 mV in the presence or absence of Cd^{2+}. Assay-validation studies showed a Z-factor of 0.83 and 0.73 on separate days. (**B**) Structures of representative compounds. *Top:* Structures of top five 'hit' compounds identified in the IWB screen of 772 FDA-approved compounds (ENZO Life Sciences). *Bottom:* Representative structures of compounds known to inhibit other CLC channels (4–5) but found to be ineffective inhibitors of CLC-2 in our screen. DPC and NFA, like the 'hit' compound MCFA, are NSAIDs.

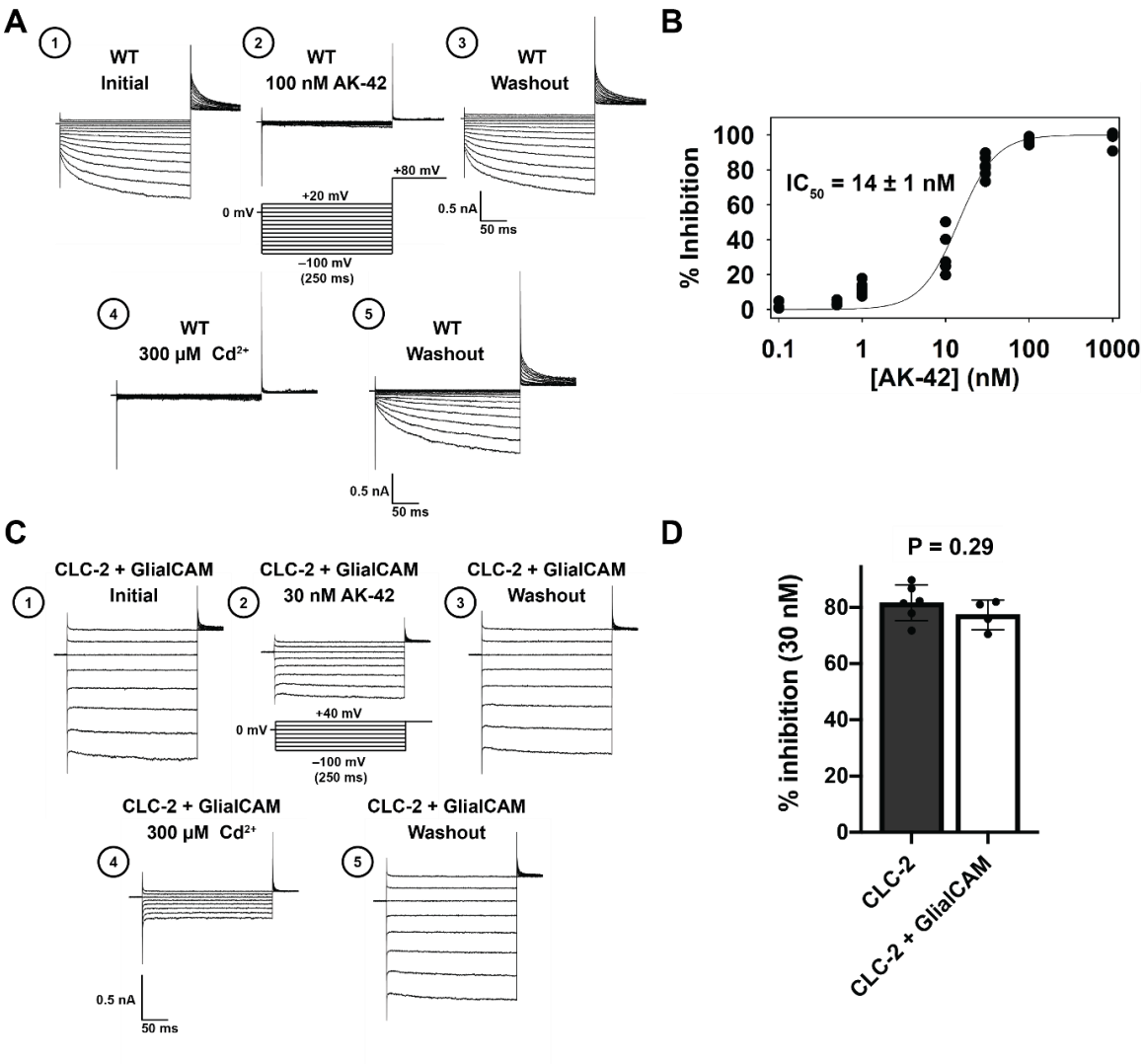

Fig. S2. Manual patch-clamp recording of rat CLC-2. (**A**) Representative traces showing rat CLC-2 currents in transiently transfected CHO cells in response to the voltage protocol shown: before, after, and following washout of 100 nM AK-42. A saturating concentration of Cd^{2+} (the low-potency CLC-2 inhibitor used in assay development, **Figure S1**) was added at the end of each experiment (Step 4) to facilitate subtraction of background currents on a given cell; Cd^{2+} was subsequently washed out (Step 5). Steps 1–5 of a typical experiment are shown. (**B**) Summary inhibition data for AK-42 against rat CLC-2, according to protocol shown in (**A**). Individual data points are shown for inhibition at –100 mV for 0.1 nM (n = 3), 0.5 nM (n = 3), 1 nM (n = 5), 10 nM (n = 5), 30 nM (n = 6), 100 nM (n = 4), 1 µM (n = 4). The fitted IC_{50} value (14 ± 1 nM) is comparable to that obtained for human CLC-2 in the IWB assay (17 ± 1 nM at –120 mV). (**C**) Representative traces showing rat CLC-2 co-expressed with GlialCAM in transiently transfected CHO cells in response to the voltage protocol shown before, after, and following washout of 30 nM AK-42. A saturating concentration of Cd^{2+} was added as in (**A**) to evaluate background currents. (**D**) Summary of inhibition data for 30 nM AK-42 against CLC-2 expressed alone (n = 6, as in **A**) or with GlialCAM (n = 4, as in **C**). Percent inhibition at –120 mV is shown for individual points. Average inhibition is not statistically different between WT CLC-2 with and without GlialCAM (P = 0.29 by unpaired t-test).

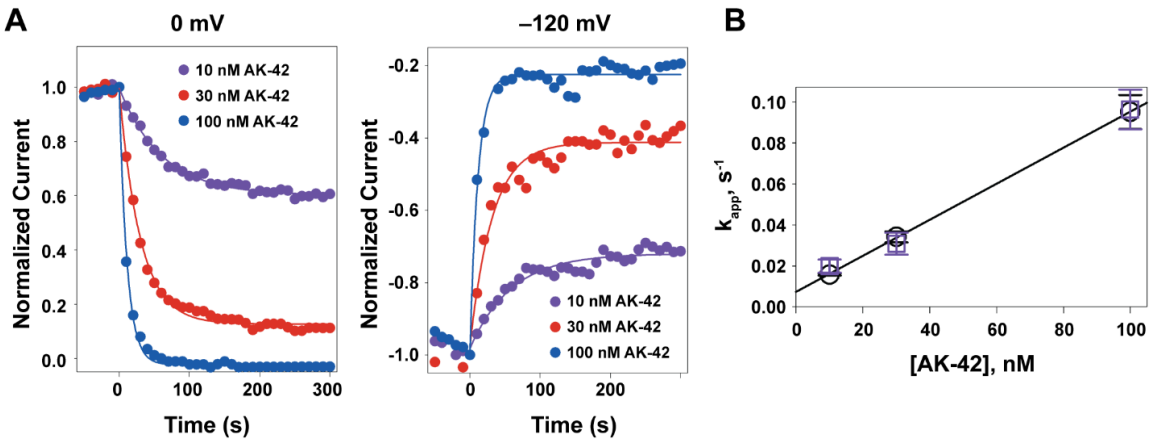

Fig. S3. Kinetics of CLC-2 inhibition. (**A**) Representative data showing the time course of CLC-2 inhibition by 10, 30, or 100 nM of AK-42. Currents were measured using the IWB; cells were held at the reversal potential (–30 mV), and currents were measured with 2-s test pulses to –120 mV followed by 0.5-s tail pulses to 0 mV, every 10 s. The peak current amplitudes in both the test and tail pulses were measured and plotted as a function of time. Data were fitted with a single exponential function to obtain values for k_{app} (apparent rate constant). (**B**) Plot of k_{app} values as a function of AK-42 concentration at –120 mV (purple) or 0 mV (black) for n = 3 (10 nM) or n = 4 (30 nM, 100 nM) cells. The linear relationship between k_{app} and AK-42 illustrates that inhibition is a first-order process, involving a 1:1 CLC-2 subunit/AK-42 interaction. Regression analysis (fitting simultaneously to both sets of points) yields estimates for on- and off-rates of 9×10^5 M^{-1} s^{-1} (slope) and 8×10^{-3} s^{-1} (intercept). While the IWB is not set up to allow measurements of reversal, we confirmed reversibility of inhibition using manual patch-clamp recordings (**Fig. S2**), with reversal occurring within ~10 min, consistent with the off-rate estimated using the IWB.

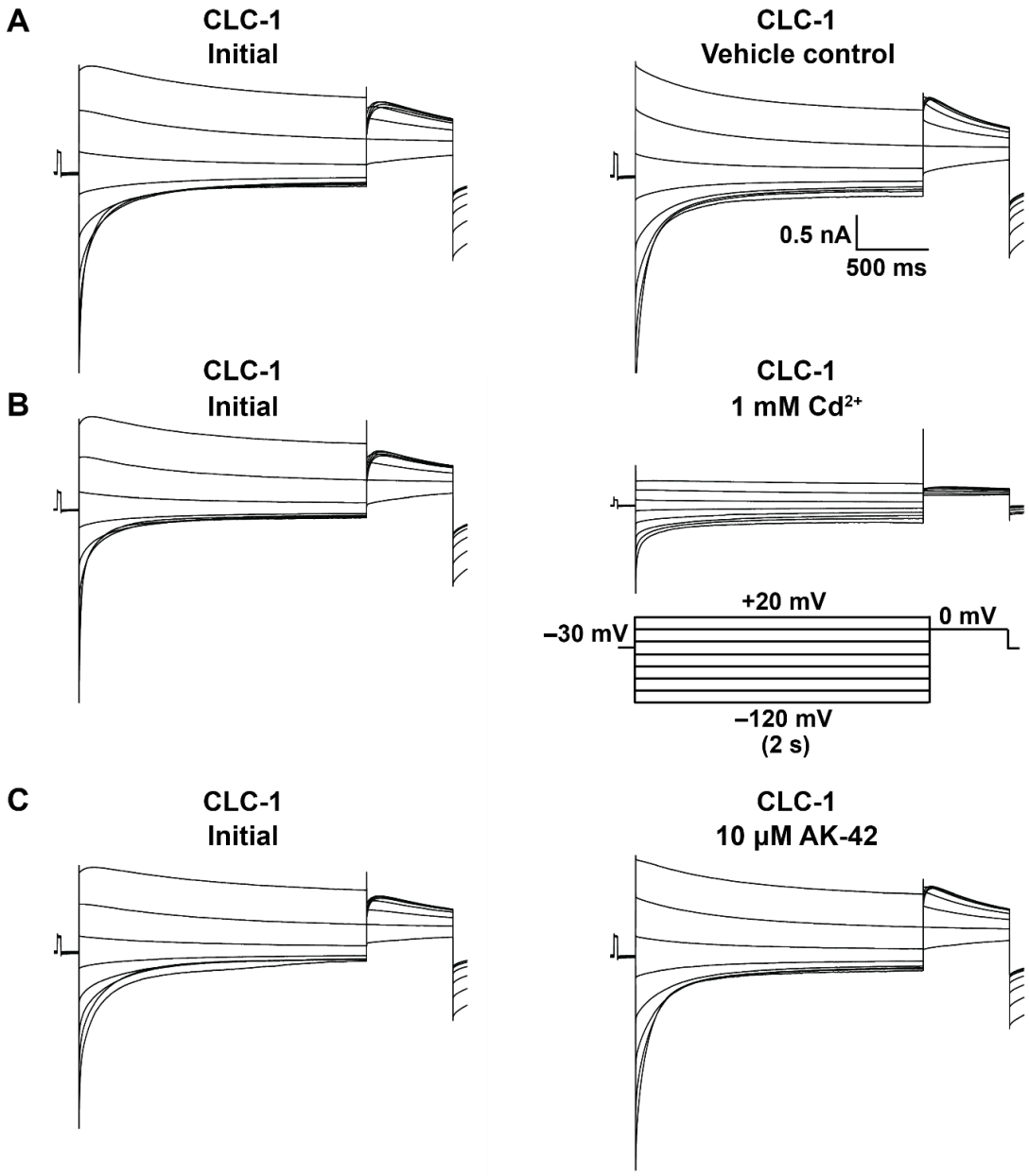

Fig. S4. IWB recordings of the CLC-1 channel for AK-42 selectivity studies. Representative traces of CLC-1 currents in a stably expressing CLC-1 CHO cell line using the IWB platform. *Left:* Currents of individual cells before application of a test article in response to the voltage protocol shown. *Right:* Response of each cell to vehicle control (0.3% DMSO in recording solution, *top*), positive control (1 mM Cd^{2+}, *middle*), or 10 µM of AK-42 (*bottom*).

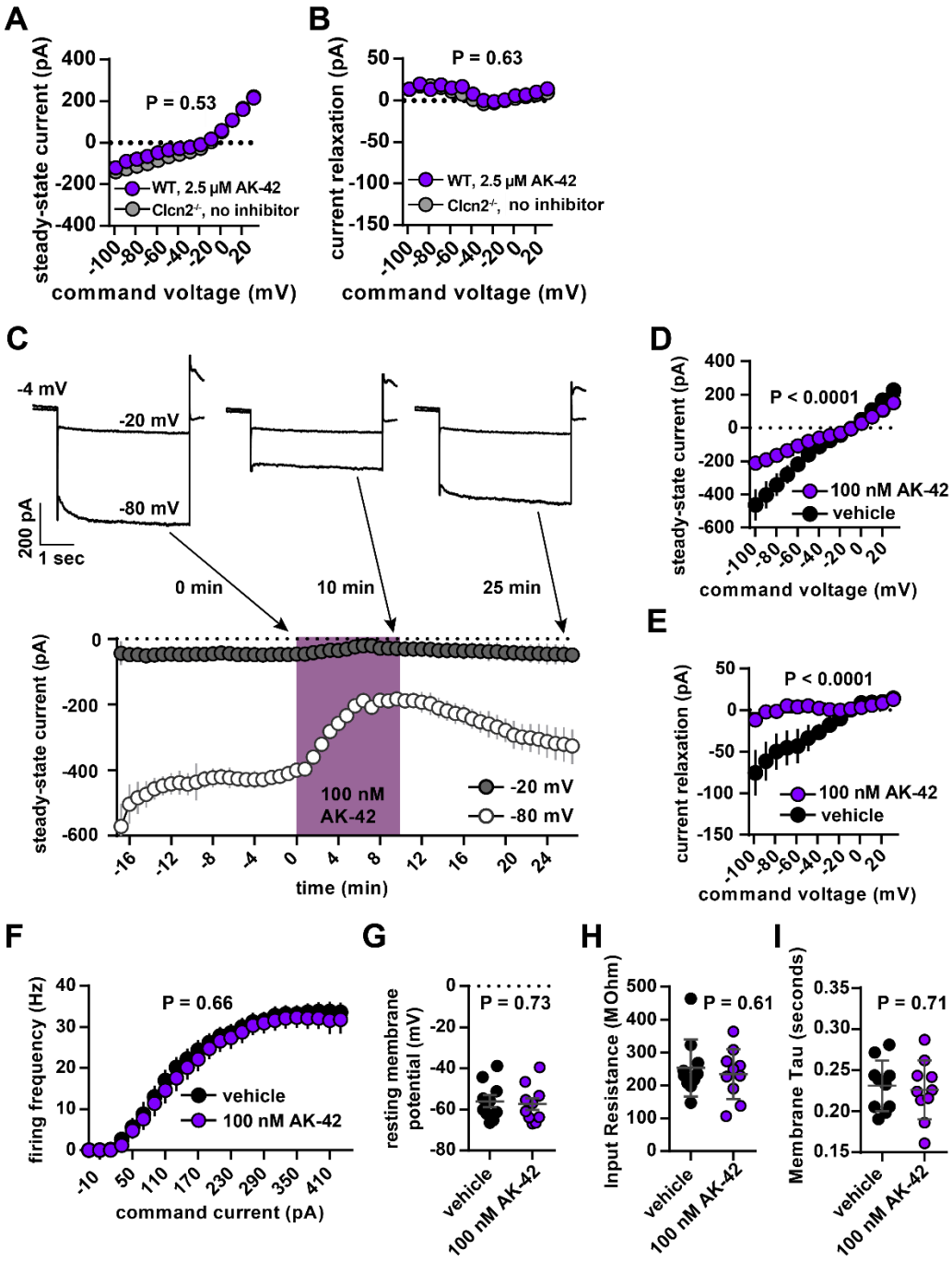

Fig. S5. Confirmation of AK-42 efficacy and specificity in brain slice recordings.

(**A–B**): **AK-42 mimics knockout of CLC-2 in CA1 neurons.** Steady-state currents (**A**) and current relaxation measurements (**B**) are indistinguishable between CLC-2 wild-type cells treated with 2.5 µM AK-42 and untreated *Clcn2*$^{-/-}$ (P = 0.53 and 0.63 for **A** and **B**, respectively via two-way RM ANOVA.).

(**C**): **Time course of CLC-2 inhibition by AK-42 at 100 nM.** Time course (bottom) and representative whole-cell current traces (top) show reversible inhibition of CLC-2 by 100 nM AK-42. Note that AK-42 visibly decreases current at hyperpolarized (–80 mV) but not depolarized (–20 mV) potentials. CLC-2 is not activated to a great extent at –20 mV; thus, this a measure of compound specificity. Capacitive transients are clipped for display purposes.

(**D–E**) **AK-42 effectively blocks CLC-2 currents at 100 nM in wild-type CA1 neurons.** Summary data showing I-V relationship of wild-type whole-cell steady-state currents (**D**) and current relaxation (**E**) before and after 10 minutes of AK-42 treatment at 100 nM (n = 6 cells, 6 slices and 6 animals. $P < 0.0001$ via two-way RM ANOVA). These results recapitulate those seen with higher (2.5 µM) concentrations of AK-42 (**Figure 5**).

(**F–I**): **Specificity of AK-42 as evidenced by lack of effects on firing frequency and membrane parameters.** (**F**) Firing frequency of CA1 pyramidal cells in response to a 500-ms current injection is not changed after the application of 100 nM AK-42 for 10 minutes. Error bars represent ± SEM throughout. ($P = 0.66$ via two-way RM ANOVA. n = 10 cells, 10 slices from 6 animals). (**G–I**) Membrane parameters remain unchanged after 10 minutes of AK-42 application (100 nM), calculated from current-clamp recordings in panel F. ($P = 0.73$, 0.61, and 0.71, respectively, via Student's unpaired *t*-test.)

Table S1. Selected initial 'hit' compounds from ENZO library screen. Summary inhibition data for initial 'hit' compounds (>20% inhibition of CLC-2 at –120 mV) and for selected NSAIDs and AT_1 antagonists sampled from the ENZO library. Percent inhibition of CLC-2 current by 30 µM compound at –120 mV is shown for each of two cells. Results from the complete screen (including those shown here) are available in **Dataset 1**. Approximate IC_{50} values of the most potent hit compounds and other selected compounds are shown in the lower right portion of the table. Values were estimated from inhibition measured at 4 concentrations of compound (1, 3, 10, 30 µM, n = 3–4 per concentration) using the IWB platform. For compounds that exhibit little or no inhibition of CLC-2, the IC_{50} is listed as > the highest concentration of compound tested, and the amount of inhibition observed at this concentration is shown in parentheses.

Entry	Compound	% (cell 1)	% (cell 2)
49	Riluzole	20	24
67	Amoxapine	25	26
80	Olmesartan	13	12
82	Olanzapine	56	54
91	Candesartan	12	13
94	Escitalopram	23	25
95	Eprosartan	10	9
127	Clozapine	62	60
136	Indomethacin	–6	10
137	Naproxen	11	15
138	Ibuprofen	9	6
144	Piroxicam	22	19
147	Ketoprofen	2	14
148	Meloxicam	21	23
165	Sulindac	10	11
168	Zafirlukast	27	30
182	Clindamycin Palmitate	20	21
210	Aspirin	16	5
240	Citalopram	19	22
244	Clobetasol Propionate	27	24
253	Diclofenac	10	15
255	Diflunisal	25	27
266	Fenoprofen	10	ND
294	Losartan	14	14
297	Mefenamic acid	ND	13
325	Progesterone	29	29
338	Spironolactone	24	19
343	Telmisartan	3	7
433	Bromfenac	2	2

Entry	Compound	% (cell 1)	% (cell 2)
473	Cisplatin	68	65
546	Etodolac	5	8
576	Hexachlorophene	42	40
586	Iloperidone	33	27
588	Irbesartan	26	29
620	Meclofenamate	84	86
647	Micafungin	27	28
687	Pazopanib·HCl	37	ND
739	Silver sulfadiazine	70	70
792	Valsartan	4	12
800	Ziprasidone	40	35

IC_{50} values for selected compounds

Entry	Compound	IC_{50} (µM)
82	Olanzapine	20
127	Clozapine	15
136	Indomethacin	>120 (0%)
253	Diclofenac	>363 (5%)
473	Cisplatin	27
620	Meclofenamate	14
739	*Silver sulfadiazine	<1
--	Aceclofenac	>429 (20%)
--	BIM1	>123 (0%)
--	BIM4	>96 (7%)
DPC	*N*-phenylanthranilic acid	>312 (27%)
--	Lubiprostone	>120 (5%)
NFA	Niflumic acid	>120 (0%)
--	Salsalate	>120 (1%)
--	*Sodium sulfadiazine	>169 (3%)

*While silver sulfadiazine exhibits a low IC_{50}, subsequent screening of the equivalent sodium salt revealed that inhibitory effects on CLC-2 are due to the silver cation and not the organic sulfadiazine scaffold, thus excluding this compound from further SAR studies.

Table S2. CLC-1 vs. CLC-2, IC_{50} values for MCFA and derivatives. Final IC_{50} values for selected compounds against human CLC-1 and human CLC-2, using the IWB platform. If the IC_{50} was greater than the highest concentration tested, this concentration is listed along with the % inhibition at this concentration (in parenthesis). *For MCFA, the maximum inhibition of CLC-1 at 100 µM was 61%; thus, this IC_{50} value is an approximation.

Compound	IC_{50} (CLC-2)	IC_{50} (CLC-1)
MCFA	7 ± 1 µM	~50 µM*
AK-24	1.2 ± 0.2 µM	>30 µM (25%)
AK-33	3 ± 1 µM	>30 µM (5%)
AK-42	0.017 ± 0.001 µM	>100 µM (22%)

Table S3. Percent inhibition of CLC-1 and CLC-2 currents with AK-42. % inhibition values for human CLC-1 and human CLC-2 with AK-42, as shown in **Figure 3**. Values of over 100% reflect that some current measurements at –120 mV flipped from negative to slightly positive in the presence of inhibitor.

Concentration (μM)	% inhibition, CLC-1	% inhibition, CLC-2
0.0003	–2 ± 6 (n = 4)	–1 ± 6 (n = 4)
0.001	1 ± 6 (n = 4)	3 ± 3 (n = 4)
0.003	3 ± 3 (n = 4)	15 ± 4 (n = 4)
0.01	2 ± 3 (n = 4)	32 ± 4 (n = 4)
0.03	–2 ± 2 (n = 8)	67 ± 2 (n = 8)
0.1	0 ± 2 (n = 7)	86 ± 1 (n = 8)
0.12	not determined (nd)	90 ± 5 (n = 4)
0.3	–2 ± 1 (n = 7)	95 ± 2 (n = 8)
1	–4 ± 2 (n = 7)	100.0 ± 0.3 (n = 8)
1.2	nd	105.1 ± 0.7 (n = 4)
3	4 ± 2 (n = 4)	100.3 ± 0.4 (n = 4)
10	5 ± 2 (n = 4)	100.3 ± 0.4 (n = 4)
12	nd	104.0 ± 0.8 (n = 3)
30	7 ± 3 (n = 4)	100.3 ± 0.3 (n = 4)
100	22 ± 2 (n = 4)	99.1 ± 0.2 (n = 4)
120	nd	106.3 ± 0.5 (n = 4)

Table S4. Inhibition of CLC-2 point mutants at 30 nM AK-42. % inhibition values for WT CLC-2 and four mutants (K400R, Q399P, K210M, K210R) with 30 nM AK-42 at –100 mV, as shown in **Figure 4D**.

CLC-2 plasmid	% inhibition
WT	82 ± 3 (n = 6)
K400R	82 ± 13 (n = 3)
Q399P	17 ± 5 (n = 3)
K210M	23 ± 9 (n = 3)
K210R	27 ± 8 (n = 3)

References Cited:

1. L. Zúñiga *et al.*, The voltage-dependent CLC-2 chloride channel has a dual gating mechanism. *J. Physiol.* **555**, 671–682 (2004).

2. Y. R. Yusef *et al.*, Removal of gating in voltage-dependent CLC-2 chloride channel by point mutations affecting the pore and C-terminus CBS-2 domain. *J. Physiol.* **572**, 173–181 (2006).

3. M. Pusch, S. Jordt, V. Stein, T. J. Jentsch, Chloride dependence of hyperpolarization-activated chloride channel gates. *J. Physiol.* **515**, 341–353 (1999).

4. A. K. Koster *et al.*, A selective class of inhibitors for the CLC-Ka chloride ion channel. *Proc. Natl. Acad. Sci.* U. S. A. **115**, E4900–E4909 (2018).

5. A. S. Verkman, L. J. Galietta, Chloride channels as drug targets. *Nat. Rev. Drug Discov.* **8**, 153–171 (2009).